Measurement of Glass Transition Temperatures in Freeze Concentrated Solutions of Non-Electrolytes by Electrical Thermal Analysis

Lih-Min Her,[1] Raymond P. Jefferis,[2] Larry A. Gatlin,[3] Bryan Braxton,[3] and Steven L. Nail[1,4]

Received November 4, 1993; accepted March 1, 1994

The electrical resistance (R) of frozen aqueous solutions was measured as a function of temperature in order to determine whether this technique can be applied for determination of glass transition temperatures of maximally freeze concentrated solutions (T_g') of non-electrolytes which do not crystallize during freezing. Electrical thermal analysis (ETA) thermograms of frozen solutions containing the solute alone show a gradual change in slope over the temperature range of interest, with no inflection point which corresponds to T_g'. However, addition of low levels (about 0.1%) of electrolyte changes the shape of the thermogram into a biexponential function where the intersection of the two linear portions of the log (R) vs. T plot corresponds to the glass transition region. The total change in log (R) over the temperature range studied increases as the ionic radius of the reporter ion increases. The sharpest inflection points in the log (R) vs T curves, and the best correlation with DSC results, were obtained with ammonium salts. T_g' values measured by ETA were compared with values measured by DSC. DSC thermograms of solutes with and without electrolyte (0.1%) show that the electrolyte decreases T_g' by about 0.5 to 1.0°C. However, T_g' values measured by ETA are somewhat higher than those measured by DSC, and difference between the two methods seems to increase as T_g' decreases. T_g' as measured by ETA is less heating rate dependent than DSC analysis, and ETA is a more sensitive method than DSC at low solute concentrations and at low heating rates. Results of electrical thermal analysis of frozen solutions are compared and contrasted with the electrical resistance vs. temperature behavior of polymer-electrolytes. ETA appears to be a useful complementary technique to DSC for characterizing formulations intended for freeze drying.

KEY WORDS: freeze drying; collapse; differential scanning calorimetry.

INTRODUCTION

During the primary drying phase of freeze drying, the frozen solution of a non-crystallizing solute must be maintained below a critical temperature, the collapse temperature. The collapse temperature is closely related to the glass transition temperature (T_g') of the maximally freeze concentrated solute (1–3). Previous work by Her and Nail examined the effects of experimental parameters on the sensitivity of differential scanning calorimetry (DSC) for T_g' measurement of aqueous solutions of several non-crystallizing solutes commonly used in freeze-dried formulations (4). While interpretation of thermal analysis data is straightforward, it is not uncommon for no glass transition to be observed in the thermogram of formulations intended for freeze drying. Possible explanations for this are that 1) the heat capacity change is too small to be measured by the instrumentation, 2) the glass transition is hidden by the leading edge of the ice melting endotherm, or 3) interactions between components of the formulation cause the glass transition region to be broadened to the extent that is not observable as a discreet change in heat capacity.

Analysis of the electrical resistance of a frozen system as a function of temperature in order to characterize formulations was introduced by Greaves in the 1950's (5), although the technique has not been systematically evaluated as a tool for formulation and process development. The principle is that charge-carrying species are relatively immobile in a thoroughly frozen system. At the onset of melting, however, the mobility of charge-carrying species increases sharply, resulting in an abrupt decrease in the electrical resistance. Electrical thermal analysis (ETA) has been shown to be a sensitive method for measuring the onset of eutectic melting for single-component solutions of inorganic salts (6) and even solutions of mannitol in water (7). However, most actual formulations crystallize incompletely or not at all, and the freeze drying characteristics are determined by the viscoelastic properties of the glassy phase. This is particularly relevant to formulations where the major component is a sugar or polyhydroxy compound which must remain amorphous in order to protect against damage to the active component by freezing, drying, or both. While it seems reasonable that electrical resistance versus temperature measurements should detect the increase in mobility of charge-carrying species as the sample is heated through the glass transition region, there are no published data which validate electrical thermal analysis (ETA) for measurement of T_g'.

The purpose of this study is to extend previous work to include the electrical resistivity versus temperature behavior of non-crystallizing, non-electrolyte solutes which have previously been characterized by DSC in order to determine the relative sensitivity of ETA for T_g' measurement, to determine the effect of experimental parameters on the results obtained from ETA measurements, and to investigate the effect of addition of low levels of "probe" ions on the electrical resistance versus temperature profile.

EXPERIMENTAL

Equipment Description

The equipment used for measurement of electrical resistance vs. temperature included a programmable cryogenic

[1] Department of Industrial and Physical Pharmacy
School of Pharmacy
Purdue University
West Lafayette, IN 47907
[2] School of Engineering
Widener University
Chester, PA 19013
[3] Parenteral and Enteral Liquid Development
Glaxo, Inc.
Research Triangle Park, NC 27709
[4] Correspondence should be addressed to:
Steven L. Nail
IPPH Department
School of Pharmacy
Purdue University
West Lafayette, IN 47907

0724-8741/94/0700-1023$07.00/0

cooler, sensors consisting of combined electrodes and resistance temperature detectors (RTDs), power supply, log resistance amplifier, and a computer for data acquisition, smoothing, and differentiation. The programmable cryogenic cooler (Cryo 10 Series, Planer Biomed Div., Middlesex, U.K.) consisted of a chamber where the temperature can be controlled from below −100°C to room temperature by means of an electrical heater, circulating fans, and metered flow of liquid nitrogen through a modulated valve into the chamber. Vials containing sample solution were placed in a test tube rack and suspended inside the chamber. The rate of heating or cooling the sample depended largely on the size of the vials. The heating rate for samples in 2 ml tubing vials was 2°C/min.

The sensor used in this study combined a platinum resistance temperature detector (RTD) and gold conductivity electrodes on separate sides of a single sensor (Model PC 320R, Hieronetics, Inc., Wallingford, PA). A schematic diagram of the sensor is shown in Figure 1. This design provides close proximity of the sensing elements to minimize errors due to temperature gradients in the sample, and prevents changes in geometry of the sensing system arising from mechanical stresses during the freezing and thawing processes. The 1000Ω RTD conforms to the DIN 43760 calibration curve.

The gauge factor, which relates measured resistance to resistivity of a material, was determined using 0.1N potassium chloride solution at 0°C. The measured gauge factor was 21.55 cm^{-1}. All data are presented as resistivity to facilitate comparison of data from different laboratories using different instrumentation.

The power supply of the resistance measurement instrumentation (Model LMS15, Hieronetics, Inc., Wallingford, PA) applies an AC potential of 1 volt at a fixed frequency of 1000 Hz. The return current from the probe is rectified and logarithmically compressed to give a dynamic range of 3–9 log ohms. The instrument is equipped with four channels to accommodate data collection from four sensors at once. Stable internal standard resistors are used, and the system self-calibrates every few seconds.

A digital low-pass filter was incorporated into the software using the algorithm $y_n = (1 - \beta)\, y_{n-1} + \beta\, x_n$, where β is a filter constant between 0 and 1, x_n is the present input, y_{n-1} is the last output, and y_n is the present output. In this study, a filter constant of 0.3 was used. Data were smoothed using a nine-point least squares method, and the first derivative of the log (R) vs. temperature curves was calculated using a 15-point algorithm as described by Savitsky and Golay (8). Software for extracting and plotting the data was provided by Hieronetics, Inc.

MATERIALS AND METHODS

The solutes examined in this study are listed in Table I. All materials were either analytical or reagent grade and were used as received. Dextran, polyvinylpyrrolidone, Ficoll® (a synthetic polymer of sucrose), and lactose were obtained from Sigma Chemical Co. Sucrose, glucose, and sorbitol were from Mallinckrodt, and trehalose was obtained from Aldrich Chemical Co. The inorganic salts used as probe electrolytes were either analytical or ACS reagent grade. Potassium chloride used for determination of the electrode gauge factor was analytical grade.

The general procedure used for electrical thermal analysis was as follows. A fixed volume (1.6 ml) of solution was filled into 2 ml glass vials. A sensor was placed in each of four vials, the vials were placed in a test tube rack, and the rack was suspended in the low-temperature chamber. The samples were cooled at a controlled rate to −50°C, held at −50°C for ten minutes to help ensure thermal equilibrium,

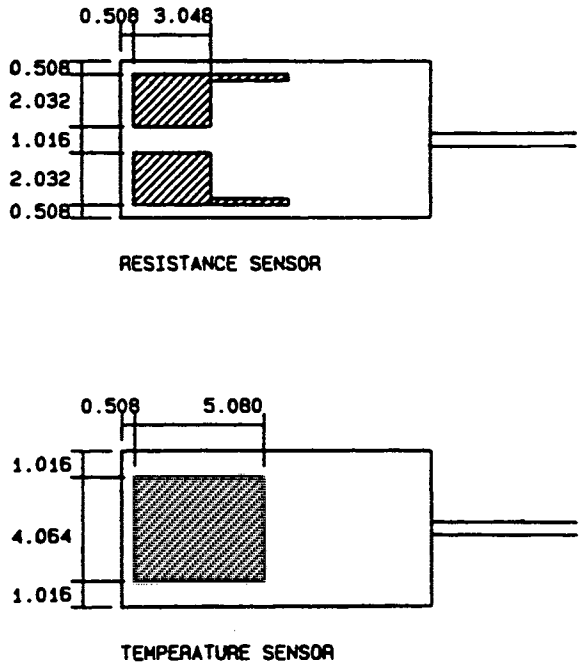

Figure 1. Schematic diagram of combined RTD and electrical resistance sensor. Dimensions are in millimeters.

Table I. ETA measured transition temperatures and heating rate corrected Tg′ values by DSC.

	ETA DATA			
10% Solution	0.1% NH_4NO_3 doped	E_1 (kJ/mole)	E_2 (kJ/mole)	DSC DATA[a]
SORBITOL	−41.6	—	140	−52.1
DEXTROSE	−40.6	—	143	−49.5
SUCROSE	−33.5	7	172	−38.7
MANNITOL	−33.7	5	128	−33.9
TREHALOSE	−31.2	6	195	−34.4
LACTOSE	−29.5	9	195	−33.4
PVP 10K	−28.3	73	135	−32.3
PVP 40K	−23.5	60	133	−26.6
FICOLL 70K	−22.6	28	215	−23.9
FICOLL 400K	−23.4	25	181	−23.9
DEXTRAN 8.8K	−14.2	60	244	−16.5
DEXTRAN 39.1K	−13.2	51	233	−15.4
DEXTRAN 70K	−13.6	47	225	−15.4
DEXTRAN 503K	−13.0	47	229	−15.0
GELATIN	−12.8	42	229	−14.2

[a] Tg′ values corrected for the effect of heating rate at 0.5 °C/min.

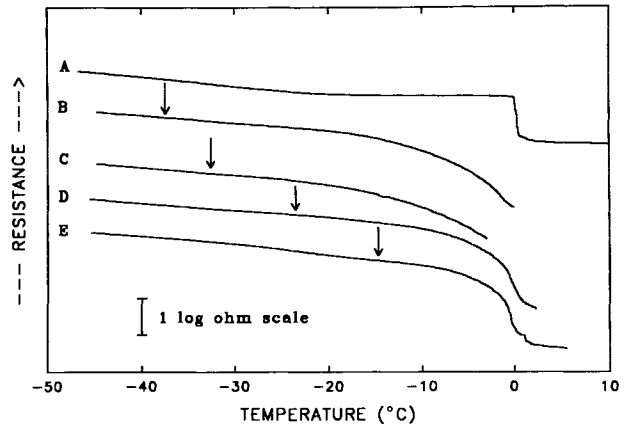

Figure 2. ETA thermograms of a) water alone and 10% aqueous solutions of b) sucrose, c) trehalose, d) ficoll (M.W. 400,000) and e) dextran (M.W. 70,000).

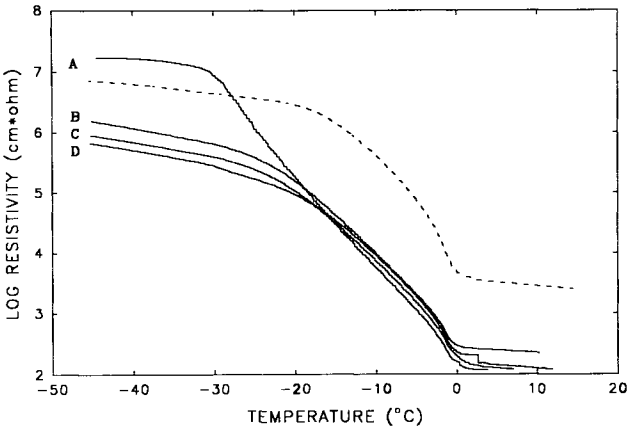

Figure 4. ETA thermograms of 10% lactose alone (dashed line) and 10% lactose containing 0.02 N a) NH_4Cl, b) KCl, c) NaCl, and d) $MgCl_2$.

then heated at a controlled rate to approximately 20°C. Log resistance vs. temperature data were collected during the warming cycle.

Differential scanning calorimetry (DSC) on frozen solutions was carried out as described previously (4).

RESULTS AND DISCUSSION

Representative ETA thermograms for non-crystallizing solutes are shown in Figure 2, along with the thermogram of distilled water. The log (R) vs. temperature profile for water is relatively flat below O°C. A sharp drop is seen at 0°C for ice, indicating that enough charge-carrying species are present to give a change in resistance of about 1 log ohm. The solutes represented in Figure 2 had previously been characterized by DSC, and the T_g' values (for the same heating rate as used in the ETA experiments) are indicated by arrows on each thermogram. The ETA thermograms are characterized by a gradual change in slope, with no clear inflection point. There is no apparent correspondence between T_g' as determined by DSC and the ETA thermogram. Of course, the data in Figure 2 are valid only for the frequency used (1000 Hz). It was not possible to study the frequency dependence of the ETA profile with the equipment used in these experiments.

The effect of doping a 10% lactose solution with low concentrations (0.02 N) of inorganic salts as probe ions is shown in Figures 3 and 4. At this concentration, none of the salts studied crystallized as a separate phase, so no eutectic melting of the salts was observed. In Figure 3, the cation is kept constant (potassium) and different anions are used. In Figure 4, the anion (chloride) is kept constant and different cations are used. Ionic radii, both crystal and hydrated, are tabulated below (9)

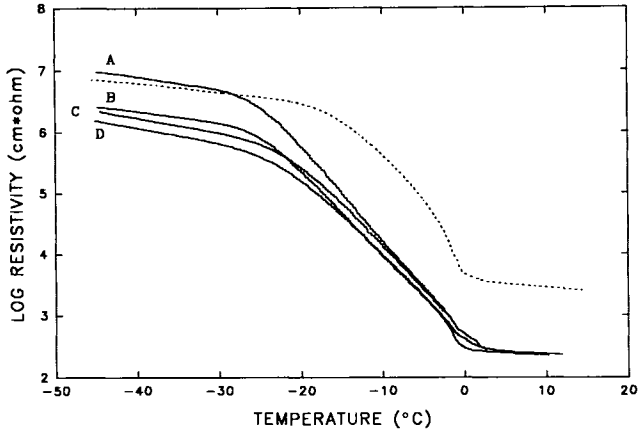

Figure 3. ETA thermograms of 10% lactose alone (dashed line) and 10% lactose containing 0.02 N a) K_2SO_4, b) KNO_3, c) KI, and d) KCl.

Ion	Ionic Radii ($\times 10^8$ cm) Crystal	Hydrated
Mg^{++}	0.65	4.28
Li^+	0.78	3.82
Na^+	0.95	3.58
K^+	1.33	3.31
NH_4^+	1.48	3.31
Cl^-	1.81	3.32
I^-	2.16	3.31
NO_3^-	2.64	3.35
SO_4^{--}	2.90	3.79

Comparing the thermograms in Figure 3 with the thermogram of lactose alone, it is seen that the effect of all of the inorganic salts is to change the shape of the thermogram to a curve with two nearly linear regions below 0°C. The change in slope occurs in the temperature range of −23°C to about −28°C for all of the salts. There is no such transition observed in the thermogram of lactose alone. The curves in Figure 3 are shown in order of decreasing anion size from top to bottom. Several observations regarding the effect of electrolyte probe on the thermogram can be made. First, the slope of the log (R) vs. temperature plot is nearly linear in the range of −20° to 0° for all of the probe electrolytes. Second, the magnitude of the resistivity at temperatures below the inflection point shows good rank order correlation with the crystal ionic radius of the anion used in the probe electrolyte; i.e., the larger the anion, the higher the resistivity in the low-temperature range.

Thermograms where the anion is constant and the cation is varied are shown in Figure 4. Again, the shape of the thermogram is changed from a smooth curve for lactose alone to two nearly linear regions with an inflection point in the range of $-25°$ to $-30°$. The thermograms are similar in the range of $-20°$ to 0°C for all of the probe electrolytes, and the resistivity below the transition temperature range again appears to correlate with the crystal ionic radius of the cation of the probe electrolyte. The sample "doped' with ammonium chloride is distinctly different from the other samples. The total change in resistivity over the temperature range examined is larger by 1–1.5 log ohms than that observed for the other salts. Also, the change in slope occurs over a narrower temperature range and at a lower temperature than for the other electrolytes. The observed transition temperature for the ammonium chloride-containing sample is at -30°C, which is in good agreement with T_g' for lactose as determined by DSC (with DSC data corrected for the slow heating rate used in the ETA experiments).

The resistivity of the sample in the temperature range below T_g' should be determined by the mobility of the probe ions in the glassy phase. While the ammonium ion has the largest crystal ionic radius of the cations studied, the observed resistivity is still higher than would be expected in comparison with radii of the other cations. Also, the table above shows that a different rank order of observed resistivity below T_g' would be expected based on the hydrated ionic radius of the electrolyte. This suggests that the state of water in the freeze concentrate is quite different than in the dilute solutions at room temperature where such radii are determined. Further studies are under way to better understand the nature of water in the freeze concentrated phase below T_g'.

Temperature Dependence of Resistivity Above and Below T_g'

Ammonium salts—particularly ammonium chloride and ammonium nitrate—consistently gave the sharpest "break" in the thermogram in the temperature range which correlates with T_g' values measured by DSC. The effect 0.1% ammonium nitrate on the ETA thermograms of several non-crystallizing, non-electrolyte solutes is shown in Figure 5. In contrast to the data in Figure 2, all of the thermograms have a sharp transition which appears to correlate reasonably well with T_g' as determined by DSC. Replotting the data according to the Arrhenius equation (log(resistivity) vs. 1/T) shows that the resistance versus temperature profile can best be treated as two Arrhenius equations; $\sigma = A_1 \exp(-E_1/RT)$ in the sub-T_g' range and $\sigma = A_2 \exp(-E_2/RT)$ above T_g'. Table I summarizes the values of T_g' as measured by ETA at a heating rate of 0.5°C/min with ammonium nitrate at 0.1% as a probe electrolyte, along with values of the activation energies E_1 and E_2.

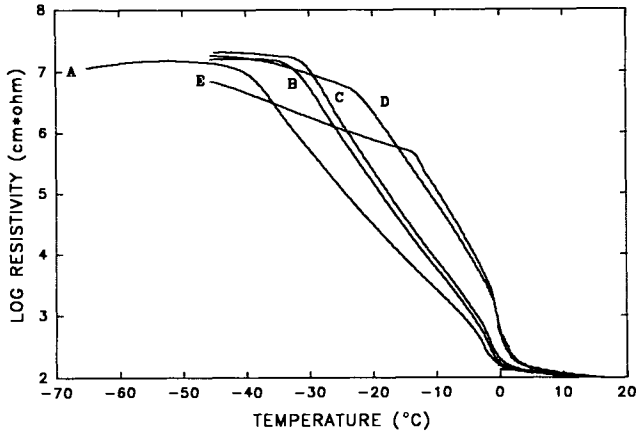

Figure 5. ETA thermograms of 10% a) sorbitol, b) sucrose, c) trehalose, d) ficoll, and e) dextran "doped" with 0.1% ammonium nitrate.

For many amorphous polymer-electrolyte systems, the temperature dependence of electrical conductivity follows the Vogel-Tammann-Fulcher (VTF) relationship (10–11).

$$\sigma = A\, T^{-1/2} \exp\left[-E_a/k\,(T—T_0)\right]$$

where σ is the electrical conductivity, A is a pre-exponential factor, E_a is the activation energy, T_0 is the ideal (zero entropy) transition temperature, and k is Boltzman's constant. The characteristic feature of VTF-type conductivity is that the conductivity increases dramatically at temperatures slightly above T_g, and increases more gradually as the temperature increases further above T_g. The data reported here are not consistent with VTF-type temperature dependency.

The VTF relationship was originally developed as an empirical equation to describe the dependence of viscosity and other transport properties of supercooled liquids on temperature. In polymer electrolyte systems, the conductivity and viscosity follow the Walden relationship, $\eta\, D \sim$ constant, where η is the viscosity and D is the diffusion coefficient of ions in solution (11). The observation of VTF type conductivity behavior of the polymer electrolyte system results from the close relationship between its viscosity and its conductivity. The temperature dependence of the viscosity of sorbitol (12) and maltose-water solutions (13) is also well described by the VTF equation. While ionic mobility in freeze concentrated solutions would be expected to be strongly influenced by viscosity, the relationship between solution viscosity and ionic mobility is not simple. The ionic conductance (λ) in aqueous mannitol, sucrose, or glycerol solutions follows, instead of the Walden relationship, the empirical relationship $\lambda\, \eta^x =$ constant, where x is less than unity and depends on the composition of the solution (14). Another complicating factor is that the composition of the freeze concentrate is not constant above T_g', since ice begins to melt immediately after heating the material through T_g'. Thus, the viscosity of the freeze concentrate above T_g' decreases not only because of increased temperature, but also because the freeze concentrate becomes more dilute. Based on this, the observed resistance of the freeze concentrate would be expected to decrease with increasing temperature more rapidly than would be predicted by the VTF equation, which is consistent with the data reported here.

Double Arrhenius type electrical conductance is observed in some polymer electrolyte systems. Armand, et al. (15) observed this type of temperature dependence in poly (oxyethylene) doped with sodium isothiocyanate, although both regions of the double Arrhenius relationship ocurred above T_g, and the higher activation energy occurred in the lower temperature range. Sharma, et al. (16), observed dou-

ble Arrhenius behavior with polyvinyl butyral (PVB) doped with an organic compound, leucomalachite green. In this system, the intersection of the two Arrhenius lines corresponds to the glass transition temperature of PVB, and E_a below T_g is less than E_a above T_g. These observations are consistent with the data reported here.

Activation energies for ionic conduction below the glass transition temperature of 10% lactose doped with various inorganic salts are in the range of 10 to 20 kJ/mole, whereas activation energies above T_g' are about an order of magnitude higher—in the range of 165–210 kJ/mole. For polymer electrolytes, a dynamic disorder hopping model has been proposed to explain conduction below the glass transition temperature (11,12). Ionic conduction in glassy materials is generally explained by the existence of defects, an ion motion is fixed by the "hopping rate" of ions between neighboring sites. The high resistance in the sub-T_g' region results from the small amount of open channels in the glass and a slow renewal rate. For the polymeric solutes used in this study, the E_1 values range from 35 kJ/mole to 80 kJ/mole, which is much larger than E_1 values for the low molecular weight solutes. This may arise because holes with sufficient volume to allow ion passage are generated more efficiently as temperature increases in the polymer solutions. The values of E_2 reported in Table I are consistent with activation energies for shear viscosity previously reported by Her and Nail (4).

Electrolyte-Induced Changes in T_g'

DSC experiments were carried out using solutes containing 0.1% ammonium nitrate compared with solutions of solute alone in order to determine whether changes were observed in the glass transition temperature resulting from the presence of the electrolyte. Representative thermograms are shown in Figure 6. In general, the effect of the electrolyte is to decrease T_g' by about 0.5–1.0°C. The largest effect was observed for Ficoll®, for which T_g' decreased by nearly 2°C. For the purposes of formulation characterization and freeze dry cycle development, this is not a serious bias. However, incorporation of electrolytes at a higher concentration results in substantial depression of T_g'. Electrolyte-induced changes in the glass transition temperature of freeze concentrated, non-crystallizing solutes will be the subject of a separate report.

Comparison of ETA with DSC for T_g' Measurement

Previous DSC studies have shown that heating rate is an important experimental parameter affecting both the observed midpoint of the glass transition and sensitivity of DSC to detection of the transition. A linear relationship was observed between ln[heating rate] and $1/T_g'$ in the range of 2°C to 20°C/min. In general, heating rates lower than 2°/min did not result in a detectable transition.

For ETA experiments, lower heating rates were necessary because of the much larger volume of sample used. The effect of heating rate on T_g' measurement by ETA was examined at heating rates of 0.1, 0.2, 0.5, 1.0, and 2.0°C/min. Observed "break points" in the curves were within about 1°C, indicating at most a very small effect of heating rate on the observed thermogram.

Direct comparison of DSC with ETA with regard to the observed transition temperature was complicated by the dif-

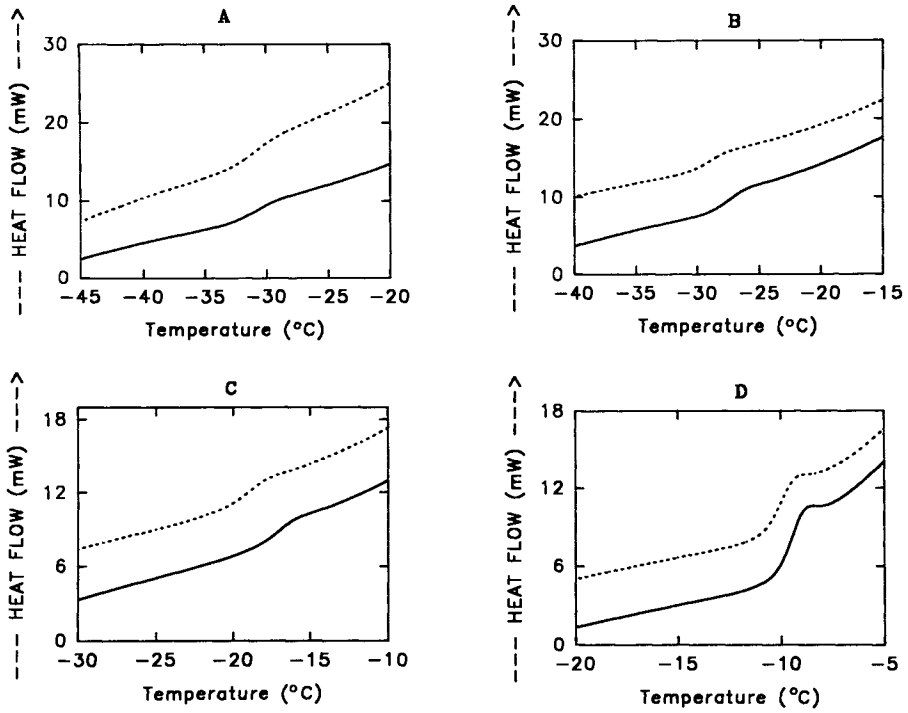

Figure 6. DSC thermograms of representative solutes with (dashed line) and without (solid line) 0.1% ammonium nitrate: a) 10% sucrose, b) 10% trehalose, c) 10% Ficoll® 400K, and d) 10% dextran 70K.

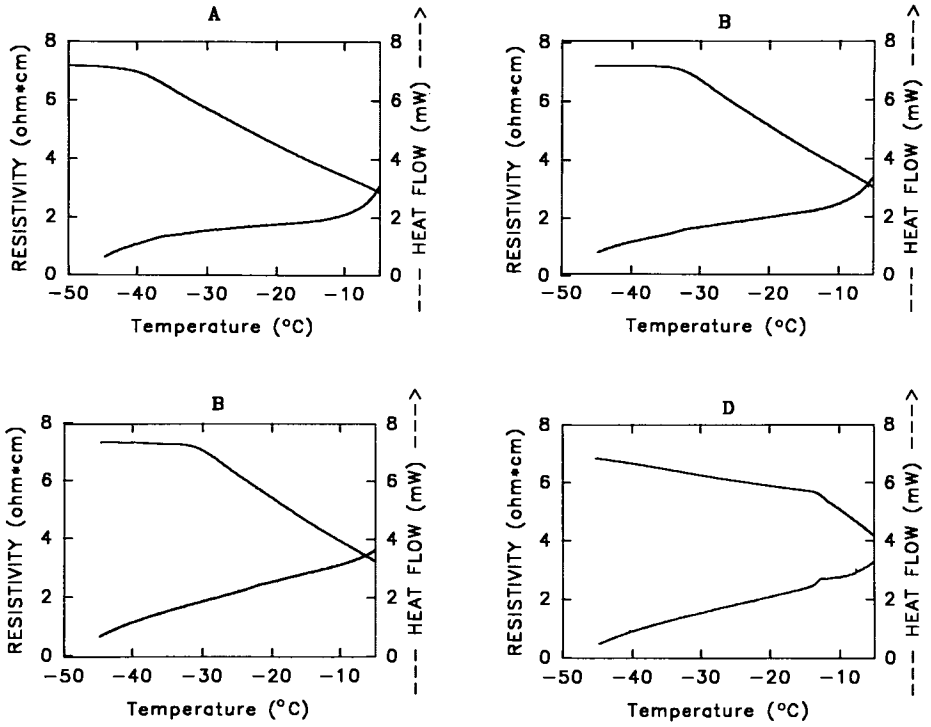

Figure 7. Comparison of ETA with DSC analysis for 10% solutions of a) sucrose, b) trehalose, c) ficoll, and d) dextran at a heating rate of 0.5°C/min. Top curve; first derivative of log(resistivity) vs. temp: Bottom curve; DSC thermogram. The samples contain 0.1% ammonium nitrate.

ferent heating rate ranges employed. However, Table I summarizes the observed transitions by both methods, where the DSC data are corrected for a heating rate of 0.5°C/min using the linear relationship between ln [heating rate] and $1/T_g'$. For nearly all solutes examined the T_g' value determined by ETA is higher than the value calculated from DSC data. The magnitude of the discrepancy between the two methods appears to depend on T_g', with the largest discrepancy observed at the lowest transition temperatures.

Glass transition temperatures measured by ETA should not be expected to be the same as those obtained by DSC, since the methods are sensitive to different kinds of motion within the materials. ETA measures movement of charge-carrying species, whereas DSC measures changes in heat capacity caused by molecular motion within the material. The magnitude of the discrepancies between T_g' values measured by DSC and ETA would not be expected to have any influence on lyophilization cycle development except when T_g' is below about −40°C. For compounds such as sorbitol and dextrose, the discrepancies are substantial, and might lead to different conclusions about the feasibility of being able to maintain the product temperature below T_g' with commercial freeze drying equipment.

The effect of cooling rate on estimation of T_g' by ETA was examined by cooling representative samples at rates of 0.1, 0.5, and 2.0°C/min before heating at 0.5°C/min. There was no significant effect of cooling rate on the subsequent ETA curve, the differences being within experimental error (about ± 0.5°C). Similarly, there was not a measureable effect of cooling rate on observed transitions by DSC unless the solute tended to crystallize with freezing.

Figure 7 illustrates a comparison of the sensitivity of ETA with DSC for T_g' measurement using four different solutes at a heating rate of 0.5°C/min. The only solute for which a glass transition is detected by DSC at this low heating rate is dextran. In contrast, the transition appears to be readily detected by ETA.

Further work is needed to determine the frequency dependence of the electrical resistance and to examine the nature of water in the freeze concentrated glass phase. However, the results of this study clarify the significance of electrical resistance measurements of formulations intended for freeze drying and show that such measurements are useful in formulation and process development of freeze dried dosage forms.

ACKNOWLEDGEMENTS

The financial support provided by the Purdue Research Foundation (LMH), Glaxo, Inc., and NIH Biological Research Support Grant #RR-05586-24 is gratefully acknowledged.

REFERENCES

1. M. J. Pikal and S. Shah. The collapse temperature in freeze drying: dependence on measurement methodology and rate of water removal from the glassy phase. Int. J. Pharm. 62:165–86 (1990).
2. A. P. MacKenzie. The physico-chemical basis for the freeze drying process. Dev. Biol. Std. 36:51–65 (1977).
3. F. Franks. Freeze drying: From empiricism to predictability. Cryo-Letters 11:93–110 (1990).
4. L. M. Her and S. L. Nail. Measurement of glass transition tem-

peratures of freeze concentrated solutes by differential scanning calorimetry. Pharm. Res. 11:54–59 (1994).

5. L. Rey. Fundamental aspects of lyophilization. In L. Rey (Ed.) *Aspects Theoretique et Industriels de Lyophilisation*, Hermann Press, Paris, 1964, pp. 24–43.
6. S. L. Nail and L. A. Gatlin. Advances in control of freeze dryers. J. Parent. Sci. Tech. 39:16–27 (1985).
7. S. L. Nail and L. A. Gatlin. Principles and practice of freeze drying. In K. E. Avis, H. A. Lieberman, and L. Lachman, *Pharmaceutical Dosage Forms: Parenteral Medications,* Vol. 2, Marcel Dekker, Inc., 1993, pp. 173–9.
8. A. Savitzky and M. J. E. Golay. Smoothing and differentiation of data by simplified least squares procedures. Anal. Chem. 36:1627–39 (1964).
9. A. L. Horvath, *Handbook of Aqueous Electrolyte Solutions—Physical Properties, Estimation and Correlation Methods*. Ellis Horwood Ltd., Chichester, U.K., 1985.
10. M. A. Ratner. Aspects of the theoretical treatment of polymer solid electrolytes: Transport theory and models. In J. R. MacCallum and C. A. Vincent (Eds), *Polymer Electrolyte Reviews, Vol I,* Elsevier Publishing Co., Amsterdam, 1987, pp. 173–236.
11. M. A. Ratner. Polymer solid electrolytes: Charge transport mechanisms. Materials Forum 15:1–15 (1991).
12. C. A. Angell, R. C. Stell, and W. Sichina. Viscosity-temperature function for sorbitol from combined viscosity and differential scanning calorimetry studies. J. Phys. Chem. 86:1540–2 (1982).
13. T. R. Noel, S. G. Ring, and M. A. Whittam. Kinetic aspects of the glass transition behavior of maltose-water mixtures. Carbohydrate Res. 212:109–17 (1991).
14. H. Sadek. Walden product, Stokes' Law and water structure—a critical review. J. Electroanal. Chem. 144:11–32 (1983).
15. J. M. Armand, M. J. Chabagno, and M. J. Duclot. Polyethers as solid electrolytes, in PIVashishta, J. N. Mundy, and G. K. Shenoy (Eds), *Fast Ion Transport in Solids*, North-Holland, New York, 1979, pp. 131–36.
16. S. K. Sharma, P. K. C. Pillai, A. K. Gupta, and M. Gupta. Effect of thermal sensitization on steady-state conductivity in polyvinyl butyral. J. Mater. Sci. Let. 6:292–4 (1987).